Impact of hemodynamic parameters on rupture risk in abdominal aortic aneurysm: Emphasis on wall shear stress-derived indicators

Harihara Maharna
University of Notre Dame
Notre Dame, IN 46556, USA

Instructor: Daniele E. Schiavazzi

Abstract

An abdominal aortic aneurysm (AAA) is the most prevalent form of aneurysm, characterized by a permanent and localized enlargement of the abdominal aorta exceeding 50% of its normal diameter, posing a high risk of rupture with a mortality rate between 70% and 90%. The global prevalence of AAA in individuals aged 30–79 is around 0.92%, and the incidence has been rising worldwide. Early detection and risk assessment, particularly of factors like thrombosis and rupture, are vital for effective treatment. The geometry and diameter of AAAs significantly affect hemodynamic forces, especially wall shear stress (WSS), which plays a crucial role in arterial remodeling and disease progression. Abnormal WSS levels can impair the arterial wall's adaptive mechanisms, making WSS-derived parameters, such as time-averaged WSS (TAWSS), oscillatory shear index (OSI), endothelial cell activation potential (ECAP), and relative residence time (RRT) essential for detailed assessment of the shear environment within an AAA. However, calculating these parameters requires a solid understanding of their physical meaning, as they are not directly computed in standard computational fluid dynamics (CFD) simulations. Recent studies focus on the relationship between these hemodynamic metrics and AAA rupture, offering valuable insights for researchers aiming to improve predictive models and intervention strategies. This review aims to explain the WSS-derived parameters, focusing on how these represent different characteristics of disturbed hemodynamics. A representative AAA model from the SimVascular repository and the virtually repaired model using SimVascular are investigated using the WSS-derived parameters. This review will be useful for understanding the physical representation of WSS-related parameters in cardiovascular flows and how they can be calculated practically for AAA investigations.

Keywords: Abdominal aortic aneurysm (AAA), time-averaged WSS (TAWSS), computational fluid dynamics (CFD)

1. Motivation

The aorta, the body's largest and most vital artery, carries blood from the heart to the rest of the organs under high pressure and velocity. Due to its critical role in circulation, any unexpected abnormalities or disorders affecting the aorta can result in severe cardiovascular complications or even death. Reflecting this serious impact, the global death rate from aortic diseases rose from 2.49 to 2.78 per 100,000 people between 1990 and 2010, highlighting the growing concern and the need for continued focus on early detection and intervention

(Bossone and Eagle, 2021; Sampson et al., 2014). One of the most common aortic disorders is the aortic aneurysm, which occurs due to an abnormal, balloon-like enlargement of the aorta. Specifically, an abdominal aortic aneurysm (AAA) is defined as a dilation of the abdominal aorta exceeding 50% of its normal diameter (McGloughlin and Doyle, 2010). Reports show that AAAs affect approximately 4–8% of men and 0.5–1% of women over the age of 50, contributing to around 15,000 deaths annually in the United States alone (Sakalihasan et al., 2005; Kontopodis et al., 2015). These statistics underscore the urgent need for early detection and appropriate medical care to reduce the risks associated with AAA progression and rupture.

Non-ruptured abdominal aortic aneurysms (AAAs) are typically silent, with most patients showing no noticeable symptoms. In fact, over 75% of individuals with an impending AAA rupture do not display any clinical warning signs (Anjum et al., 2012). Detection often occurs incidentally during routine health screenings or evaluations for other conditions, particularly in patients with coronary, peripheral, or cerebrovascular diseases (Wilmink et al., 1999). Although uncommon, some non-ruptured AAAs are identified through complications such as distal embolization or acute thrombosis, which prompt further medical investigation (Sakalihasan et al., 2005).

The rupture of an abdominal aortic aneurysm (AAA) constitutes a life-threatening surgical emergency, primarily due to internal bleeding (hematocele) and a sudden reduction in blood flow to vital organs. It represents the most critical and fatal outcome of aneurysmal disease, with an overall mortality rate reaching approximately 80%. Most cases of ruptured AAAs do not survive long enough to undergo surgical intervention, meaning that the surgeries performed represent only a small portion of the actual cases. While surgical outcomes have seen some improvement in recent years, overall survival rates remain low, and advancements have only modestly influenced these outcomes (Bengtsson and Bergqvist, 1993). Therefore, early and appropriate care for AAA detected by medical imaging modalities will significantly reduce the risk of rupture and mortality rates.

In this project, my approach to studying cardiovascular hemodynamics involves computationally evaluating the complex stresses acting on aneurysmal tissue (Mutlu et al., 2023). An AAA model has been chosen from the SimVascular repository to analyze the hemodynamic parameters. Specifically, using computational fluid dynamics (CFD) which enables detailed analysis of disturbed flow patterns and frictional shear stresses on the vessel wall. By incorporating patient-specific blood flow conditions and aortic geometry as boundary inputs, CFD solves the governing physical equations to simulate the unsteady nature of cardiovascular flows. This allows for precise assessment of velocity gradients and wall shear stress near the vessel wall. CFD has been widely applied to explore intricate flow dynamics in the aorta (Salman et al., 2021), and numerous studies have attempted to correlate CFD-derived hemodynamic parameters with AAA progression and rupture risk (Salman et al., 2019; Xenos et al., 2010; Fillinger et al., 2002). Recent reviews have also highlighted the role of CFD in rupture risk prediction (McGloughlin and Doyle, 2010; Lipp et al., 2020), while some pioneering clinical efforts have demonstrated its potential in surgery planning using patient-specific data (Lipp et al., 2020). Despite its promise, the clinical integration of CFD remains limited due to challenges in practicality, accessibility, and validation (McGloughlin and Doyle, 2010; Polzer and Gasser, 2015).

A significant challenge in the study of abdominal aortic aneurysms (AAAs) lies in accurately characterizing the unsteady and disturbed blood flow within the aneurysmal region. Hemodynamic parameters related to wall shear stress (WSS), such as time-averaged WSS (TAWSS), oscillatory shear index (OSI), endothelial cell activation potential (ECAP), and relative residence time (RRT), are essential for evaluating the complex shear environment acting on the aneurysm wall. Although recent computational studies have made notable progress in incorporating these metrics into CFD-based rupture risk assessments, calculating them is not straightforward and demands a clear physical understanding of what each parameter represents. Moreover, standard CFD solvers do not automatically compute these metrics during simulations, adding another layer of complexity (Mutlu et al., 2023). As a result, assessing AAA rupture risk through hemodynamic parameters remains a challenging task.

This review aims to clarify the significance of WSS-derived parameters by illustrating how they reflect distinct features of disturbed flow, presenting a representative case to support both spatial and temporal formulation. We have also virtually repaired the model to observe how the hemodynamic parameters are responding to the change. These insights are intended to aid researchers in practically applying these calculations in AAA investigations, ultimately enhancing our understanding of their role in rupture risk prediction (Mutlu et al., 2023)

2. Team

I am especially grateful to Dr. Daniele E. Schiavazzi for his support and encouragement throughout this project. His insightful suggestions and genuine interest in my work helped me stay motivated and think more critically. I truly appreciate the time he took to guide me.

3. Cardiovascular model

I choose a AAA model (Figure 1) from the the SimVascular repository. A finite element mesh for simulations was generated using the open-source TetGen package (Si, 2015), which is included in SimVascular. To ensure mesh convergence and achieve local accuracy near the wall, which is necessary to adequately resolve WSS, we constructed a boundary-layer mesh and used local mesh refinement in the aneurysmal regions.

Additionally, we virtually reconstructed healthy model that removes the aneurysmal deformation from the original AAA geometry using SimVascular (Figure 2).

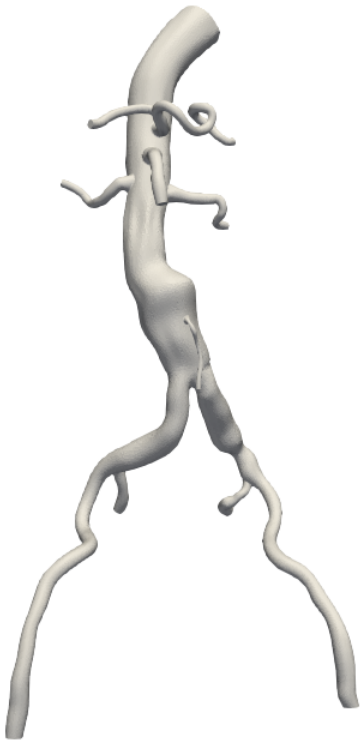

Figure 1: AAA model from SimVascular

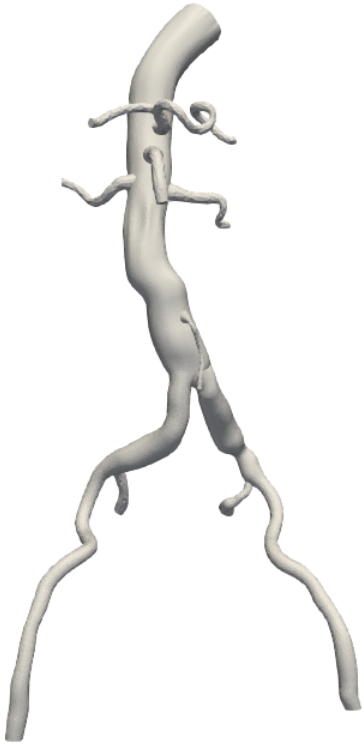

Figure 2: Virtually repaired model

3.1 Governing equations and CFD (Computational fluid dynamics) methodology

We solved the time-dependent Navier-Stokes equations using the SimVascular, which is the governing blood flow. Blood was modeled as an incompressible Newtonian fluid (density = 1.06 g/cc, dynamic viscosity = 0.04 dynes/cm^2). Boundary conditions for the blood flow (Figure 3) at inlet and outlets of the aorta were enforced using a lumped parameter network model.

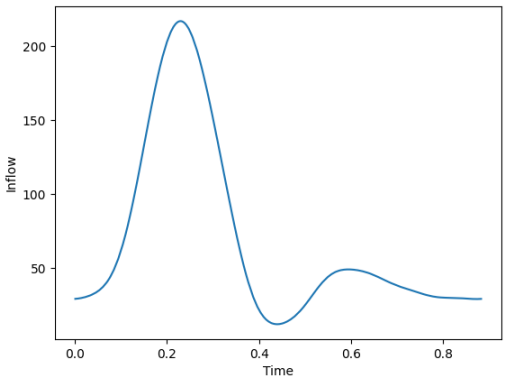

Figure 3: Inflow

4. Hemodynamic parameters

WSS vector can be obtained from the simulation output. This section describes the calculating of the WSS-related parameters and explain how these parameters can be

used in the rupture risk assessment of AAA.
A detailed calculation methodology is given
in the Mutlu et al. (2023). I have also compared the disease model and the reconstructed healthy model for all the parameters.

4.1 TAWSS (Time-averaged wall shear stress)

TAWSS is an important parameter for identifying critical regions in AAA that are susceptible to rupture, as illustrated in Figure 4 and the virtually repaired model in Figure 5. However, it has been observed that rupture locations cannot be determined solely by quantifying TAWSS levels. Other factors, such as the thickness of the ILT, also contribute significantly to the rupture mechanism (Mutlu et al., 2023).

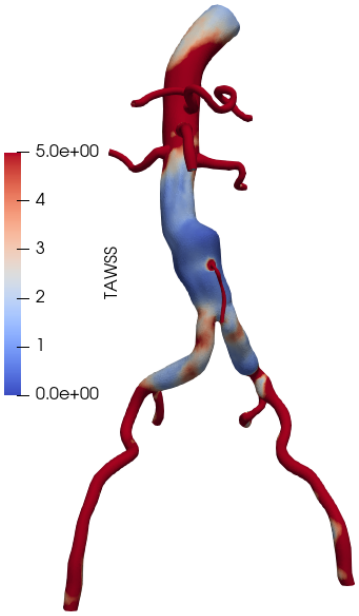

Figure 4: TAWSS of AAA model

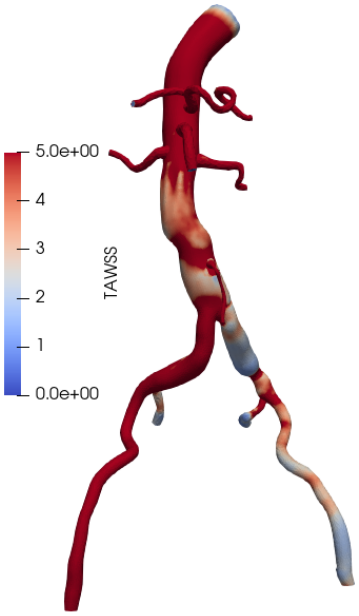

Figure 5: TAWSS of virtually repaired model

The formulation of TAWSS is defined in Eq. (1). To calculate TAWSS, the absolute values of the x, y, and z components of the wall shear stress (WSS) are used over a time period T, which typically corresponds to one full cardiac cycle. In Eq. (1), $\boldsymbol{\tau}_w$ represents the instantaneous WSS vector:

$$\text{TAWSS} = \frac{1}{T}\left(\int_0^T |\boldsymbol{\tau}_w|\, dt\right) \tag{1}$$

In many computational fluid dynamics (CFD) software packages, this TAWSS formulation is not available as a default post-processing option. As a result, these tools cannot

directly compute TAWSS values at each mesh point. To determine the TAWSS distribution on an AAA surface, the WSS vectors in three spatial directions (WSS_x, WSS_y, and WSS_z) must be extracted at each time step. Then, Eq. (1) should be implemented using an external software package (`MATLAB`, `Python`, etc.) (Mutlu et al., 2023).

4.2 OSI (Oscillatory shear index)

OSI is another critical hemodynamic parameter that explains the periodic separation of WSS from the prevailing axial direction. I have used the OSI defined in Mutlu et al. (2023). The OSI is defined as:

$$\text{OSI} = \frac{1}{2}\left(1 - \frac{\left|\int_0^T \boldsymbol{\tau}_w \, dt\right|}{\int_0^T |\boldsymbol{\tau}_w| \, dt}\right) = \frac{1}{2}\left(1 - \frac{\frac{1}{T}\left|\int_0^T \boldsymbol{\tau}_w \, dt\right|}{\frac{1}{T}\int_0^T |\boldsymbol{\tau}_w| \, dt}\right) = \frac{1}{2}\left(1 - \frac{\frac{1}{T}\left|\int_0^T \boldsymbol{\tau}_w \, dt\right|}{\text{TAWSS}}\right) \tag{2}$$

In this equation, $\boldsymbol{\tau}_w$ is the instantaneous WSS vector and T is the duration of one cardiac cycle. Figure 6 shows the OSI for the AAA model, while Figure 7 shows the OSI for the virtually repaired model. The OSI values range from 0 to 0.5, with 0 indicating fully unidirectional WSS and 0.5 indicating WSS with a temporal average of zero (Taylor et al., 1998; Les et al., 2010).

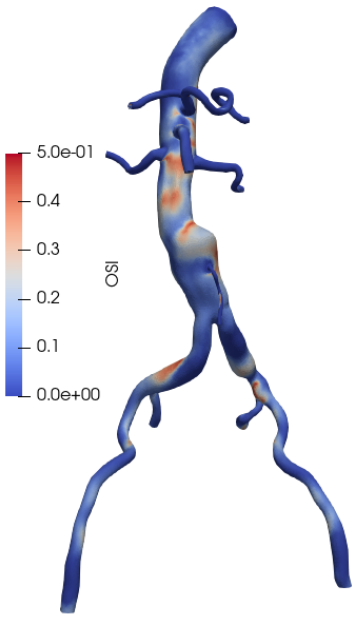

Figure 6: OSI of AAA model

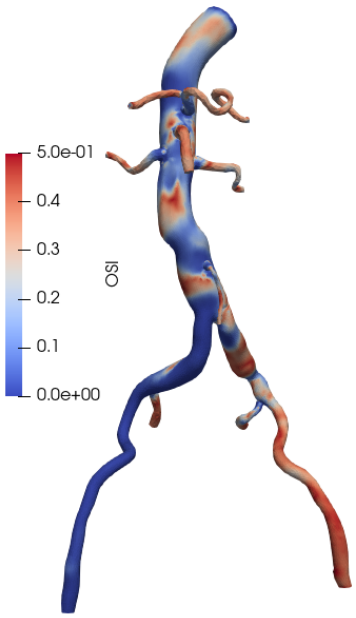

Figure 7: OSI of virtually repaired model

4.3 ECAP (Endothelial cell activation potential)

The ECAP metric, proposed by Achille et al. (2014) , uses the ratio of OSI to TAWSS to describe the thrombogenic susceptibility of the vessel wall, as shown in Eq. (3). ECAP

is used to identify regions that are exposed to high OSI and low TAWSS, as illustrated in Figure 8 for the disease model and Figure 9 for the virtually repaired model. High ECAP index values correspond to conditions of large OSI and small TAWSS, which indicate increased endothelial sensitivity:

$$\text{ECAP} = \frac{\text{OSI}}{\text{TAWSS}} \tag{3}$$

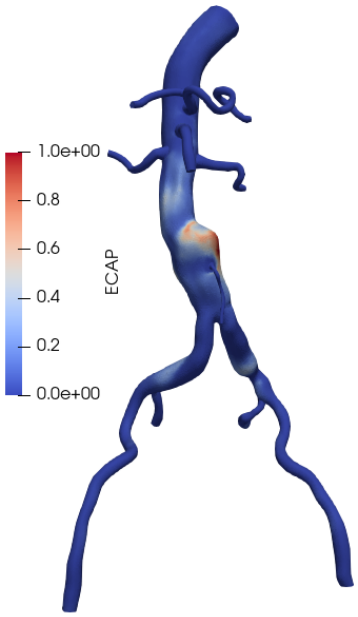

Figure 8: ECAP of AAA model

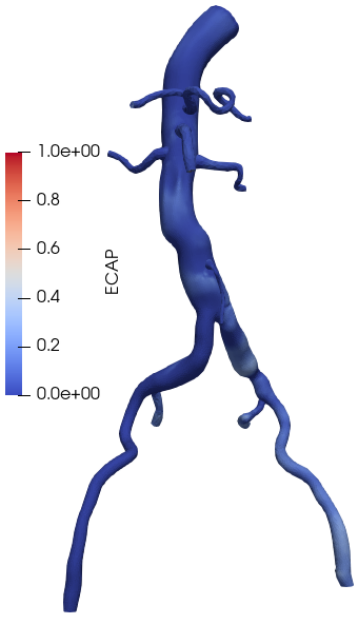

Figure 9: ECAP of virtually repaired model

4.4 RRT (Relative residence time)

According to Himburg et al. (2004), the combined analysis of Time-Averaged Wall Shear Stress (TAWSS) and Oscillatory Shear Index (OSI) provides insight into the residence time of blood near the vessel wall. This led to the introduction of a new hemodynamic metric known as the Relative Residence Time (RRT), which serves to quantify disturbed flow patterns (Himburg et al., 2004). Figure 10 shows the RRT for the AAA model, while Figure 11 shows the RRT for the virtually repaired model. Since RRT is defined as the inverse of the magnitude of the time-averaged wall shear stress vector, it demonstrates a strong correlation with TAWSS. As a result, RRT has been proposed as a potential unified indicator to replace both WSS and OSI in characterizing regions of "low and oscillatory" shear stress (Lee et al., 2009). The formal definition of RRT is presented in Eq. (4), and it should be emphasized that RRT is inversely related to the numerator of the OSI expression,

as shown in Eq. (5).

$$\text{RRT} = \frac{1}{(1 - 2 \times \text{OSI}) \times \text{TAWSS}} \tag{4}$$

$$\text{RRT} = \frac{1}{\left| \frac{1}{T} \int_0^T \vec{\tau}_w \, dt \right|} \tag{5}$$

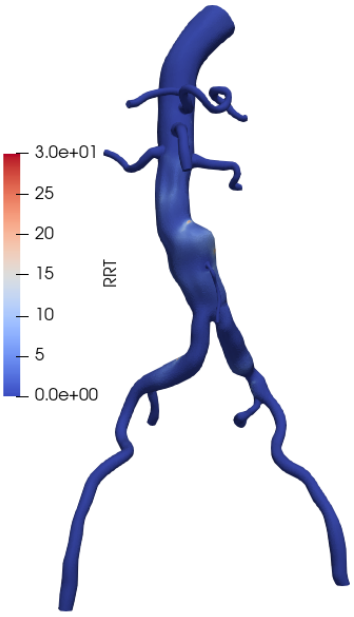

Figure 10: RRT of AAA model

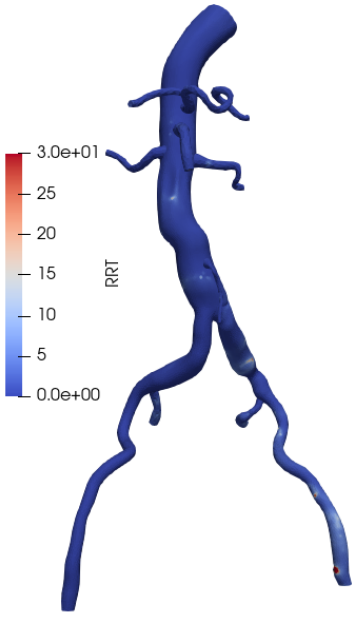

Figure 11: RRT of virtually repaired model

5. Results

In this section, I will describe the importance of hemodynamic parameters that I defined in the previous section. Evaluating WSS magnitudes at specific time points, such as at the peak flow velocity, is not sufficient for identifying the critical regions on the aneurysm sac. This limitation arises from the combined hemodynamic effects occurring throughout the entire cardiac cycle, which play a key role in aneurysm expansion or rupture. Consequently, assessing the average forces exerted on the wall during the full cardiac cycle is essential for identifying the potential rupture zones. It is important to emphasize that relying solely on TAWSS is typically inadequate for pinpointing high-risk rupture locations. Thus, incorporating multiple parameters, including OSI, ECAP, and RRT alongside TAWSS, enhances the reliability of rupture risk assessments and leads to more accurate predictive outcomes (Mutlu et al., 2023).

5.1 Effects of WSS (Wall shear stress) and TAWSS (Time average wall shear stress)

Recent studies have demonstrated that low wall shear stress (WSS) on the vessel wall is a significant risk factor associated with the development of atherosclerosis and the progression of aneurysms (Les et al., 2010; Biasetti et al., 2011). Prolonged exposure to low WSS on the aneurysm wall has been shown to increase intercellular permeability (Okano and Yoshida, 1994) and lead to severe degradation of elasticity within the aneurysm sac (Watton et al., 2009). Moreover, oscillatory and irregular WSS levels below 0.4 Pa contribute to the development of atherosclerosis by inducing endothelial cell degeneration (Malek, 1999; Taylor et al., 1999; Bappoo et al., 2021). Physiological WSS values in large arteries typically range between 1 and 5 Pa (Ene-Iordache and Remuzzi, 2012). When endothelial cells are exposed to WSS within this physiological range, anti-inflammatory and anti-thrombogenic responses are triggered, initiating the vascular remodeling process. As a result, WSS within the physiological limits positively influences vascular health (Dewey et al., 1981; Metaxa et al., 2008; Szymanski et al., 2008). In contrast, a low WSS environment may promote conditions that activate coagulation factors, enhance platelet adhesion, and lead to platelet deposition and the proliferation of intraluminal thrombus (ILT) in flow recirculation zones (Xenos et al., 2010; McClarty et al., 2021; Paszkowiak and Dardik, 2003; Reneman et al., 2006; Bluestein et al., 2009).

Although time-averaged wall shear stress (TAWSS) plays a significant role in modulating intraluminal thrombus (ILT) deposition, an increase in ILT thickness is not consistently observed in regions with low TAWSS. A reduction in TAWSS, resulting from slow circulation within the abdominal aortic aneurysm (AAA) sac, has been linked to aneurysm enlargement (Wang and Li, 2013). Furthermore, both the growth rate of AAAs (Zambrano et al., 2016) and their rupture (Forneris et al., 2020; Doyle et al., 2014) have been associated with low TAWSS and elevated ILT accumulation. Several studies indicate that aneurysm rupture in low-WSS regions (McClarty et al., 2021) correlates with ILT buildup in these areas (Qiu et al., 2019; Boyd et al., 2016), along with the presence of aortic wall hypoxia (Vorp et al., 2001; Metaxa et al., 2018), which contributes to local wall weakening and increased rupture susceptibility. Conversely, other findings suggest that high WSS levels (WSS $>$ 3 Pa (Dolan et al., 2013)) on the AAA wall are also associated with aneurysm rupture (Xenos et al., 2010; Meng et al., 2014).

5.2 Effects of OSI (Oscillatory shear index)

The phenotypic regulation of abdominal aortic aneurysm (AAA) development has been shown to correlate with high blood pressure, increased medial thickness, and elevated oscillatory shear index (OSI), all of which are linked to cellular inflammation (Meng et al., 2014; Chen et al., 2018). OSI is also associated with thrombus formation and growth, indicating a relationship between OSI and intraluminal thrombus (ILT) accumulation (Tzirakis et al., 2017). Notably, significant thrombus growth is observed in regions with low OSI values ($<$ 0.1). In contrast, regions with low TAWSS and OSI values exceeding 0.1 tend to exhibit limited or no thrombus growth (Boniforti et al., 2021; O'Rourke et al., 2012). Lozowy et al. found no direct correlation between OSI and ILT deposition in a study of 23 AAA cases with diameters exceeding 5 cm, attributing this to abnormal flow patterns in

large-diameter AAAs compared to more typical flow in smaller ones (Lozowy et al., 2017). However, Zambrano et al. reported that ILT accumulation can occur at both high and low OSI values (Zambrano et al., 2021).

The combined analysis of time-averaged wall shear stress (TAWSS) and oscillatory shear index (OSI) is essential for identifying critical regions on the vessel or aneurysm wall. Previous studies have demonstrated that the coexistence of low TAWSS and high OSI is associated with intravascular abnormalities, which are further linked to aneurysm growth and rupture (Boniforti et al., 2021; Zambrano et al., 2016; Tzirakis et al., 2017). Arzani et al. reported that thrombus growth frequently occurs in regions where TAWSS ranges between 2 and 3 dyn/cm^2, and found a significant negative correlation between OSI and thrombus accumulation. Notably, ILT accumulation is generally absent in regions characterized by high OSI values (> 0.4) combined with very low TAWSS values (< 0.1 Pa) (Arzani et al., 2014).

5.3 Effects of RRT (Relative Residence time) and ECAP (Endothelial cell activation potential)

TAWSS, OSI, and ECAP have been identified as reliable predictors for locating potential rupture sites when comparing ruptured and non-ruptured AAA surfaces. However, in some cases, using a fixed threshold for TAWSS, OSI, or ECAP to determine rupture locations may not be practical. The accumulation of intraluminal thrombus (ILT), which results from hemodynamic conditions, influences wall shear stress (WSS) on the aneurysm sac and alters the mechanical properties of the wall, including elasticity and thickness. Since these properties contribute to the likelihood of rupture in a degenerative wall, the presence and extent of ILT should also be considered in rupture risk assessments.

A recent study compared three groups of ruptured abdominal aortic aneurysms (AAAs): those without ILT, those with a thin ILT layer, and those with a thick ILT layer. In AAAs without ILT, rupture occurred in regions characterized by low TAWSS, high OSI, and high ECAP. Conversely, in AAAs with thick ILT layers, rupture was observed in areas with high TAWSS and low ECAP. Interestingly, for AAAs with a medium ILT thickness, no clear correlation was found between rupture risk and any of the three hemodynamic indicators (Qiu et al., 2019).

Studies investigating relative residence time (RRT) and endothelial cell activation potential (ECAP) have shown that the prolonged residence time in recirculation zones facilitates sufficient exposure for activated platelets to adhere to thrombogenic or atherogenic surfaces (Biasetti et al., 2010, 2011). RRT has been found to exhibit a consistent positive correlation with thrombus growth (Tzirakis et al., 2017). Kelsey et al. identified ECAP high values indicative of critical thrombus-prone regions. Additionally, regions with both the highest ECAP values and the longest residence times were found to be more susceptible to thrombus formation (Kelsey et al., 2017).

6. Conclusions and possible improvements

Disturbed hemodynamics is a well-established factor influencing the progression of abdominal aortic aneurysms (AAAs). Several parameters have been proposed to characterize disturbed hemodynamics in cardiovascular flows, with TAWSS, OSI, ECAP, and RRT be-

ing the most widely applied in AAA investigations. In this work, we have discussed these WSS-derived parameters, focusing on their ability to capture different aspects of disturbed hemodynamics. A representative case with the virtually repaired model was provided to offer a spatial and temporal formulation that could serve as a useful reference for researchers interested in practical applications. Additionally, we summarized recent findings linking WSS-related parameters with AAA rupture risk assessment.

TAWSS and OSI, as well-known WSS-related parameters, have been shown to influence endothelial sensing-mediated vascular remodeling (Shojima, 2004; Meng et al., 2007). ECAP (Achille et al., 2014), defined as the ratio of OSI to TAWSS, serves as a key indicator of the thrombogenic susceptibility of the arterial wall. RRT, a newly developed hemodynamic parameter, is used to describe the relatively slower flow characteristics near the aneurysm wall (Xiang et al., 2011).

Many studies have demonstrated that low WSS in the AAA sac leads to wall tissue degradation and ILT accumulation, which in turn reduces the mechanical strength of the arterial wall and increases rupture risk. Conversely, high WSS has also been linked to an elevated rupture risk. In small-diameter AAAs, low OSI levels facilitate ILT formation within the aneurysm sac, though OSI appears to have less effect on ILT deposition as the aneurysm diameter increases. The general consensus is that low TAWSS combined with high OSI creates abnormal conditions that may lead to AAA enlargement or rupture. The presence of ILT, however, introduces significant complexities to the problem, and the aforementioned conclusions may not hold when considering variations in the thickness and shape of the ILT (Mutlu et al., 2023).

In conclusion, WSS-related parameters are critical for characterizing cardiovascular flows and hold significant promise for assessing disease severity, particularly in the context of AAAs, where they can be used to predict rupture risk. While TAWSS, OSI, ECAP, and RRT remain the most studied parameters, newer metrics such as wall shear stress exposure time (WSSET) and time-averaged WSS divergence (WSSdiv) (Arzani et al., 2014; Arzani and Shadden, 2016; Arzani et al., 2017) are continually being introduced to more accurately represent disturbed hemodynamics in cardiovascular flows. Looking forward, advancements in computational fluid dynamics (CFD) tools and methodologies are expected to result in faster and more efficient simulations, enabling better utilization of WSS-derived parameters in clinical cardiovascular practice. These innovations could ultimately improve patient-specific risk assessments and contribute to more effective clinical decision-making in the management of AAAs.

References

P. Di Achille, G. Tellides, C.A. Figueroa, and J.D. Humphrey. A haemodynamic predictor of intraluminal thrombus formation in abdominal aortic aneurysms. *Proceedings of the Royal Society A: Mathematical, Physical and Engineering Sciences*, 470(2172), 2014. doi: 10.1098/rspa.2014.0163.

A. Anjum, R. von Allmen, and R. Greenhalgh. Explaining the decrease in mortality from abdominal aortic aneurysm rupture. *Journal of Vascular Surgery*, 56(3):876, 2012. doi: 10.1016/j.jvs.2012.07.017.

A. Arzani and S.C. Shadden. Characterizations and correlations of wall shear stress in aneurysmal flow. *Journal of Biomechanical Engineering*, 138(1), 2016. doi: 10.1115/1.4032056.

A. Arzani, G.Y. Suh, R.L. Dalman, and S.C. Shadden. A longitudinal comparison of hemodynamics and intraluminal thrombus deposition in abdominal aortic aneurysms. *American Journal of Physiology-Heart and Circulatory Physiology*, 307(12):H1786–H1795, 2014. doi: 10.1152/ajpheart.00461.2014.

A. Arzani, A.M. Gambaruto, G. Chen, and S.C. Shadden. Wall shear stress exposure time: a lagrangian measure of near-wall stagnation and concentration in cardiovascular flows. *Biomechanics and Modeling in Mechanobiology*, 16(3):787–803, 2017. doi: 10.1007/s10237-016-0853-7.

N. Bappoo et al. Low shear stress at baseline predicts expansion and aneurysm-related events in patients with abdominal aortic aneurysm. *Circulation: Cardiovascular Imaging*, 14(12):1112–1121, 2021. doi: 10.1161/CIRCIMAGING.121.013160.

H. Bengtsson and D. Bergqvist. Ruptured abdominal aortic aneurysm: a population-based study. *Journal of Vascular Surgery*, 18(1):74–80, 1993. doi: 10.1067/mva.1993.42107.

J. Biasetti, T.C. Gasser, M. Auer, U. Hedin, and F. Labruto. Hemodynamics of the normal aorta compared to fusiform and saccular abdominal aortic aneurysms with emphasis on a potential thrombus formation mechanism. *Annals of Biomedical Engineering*, 38(2):380–390, 2010. doi: 10.1007/s10439-009-9843-6.

J. Biasetti, F. Hussain, and T. Christian Gasser. Blood flow and coherent vortices in the normal and aneurysmatic aortas: a fluid dynamical approach to intraluminal thrombus formation. *Journal of the Royal Society Interface*, 8(63):1449–1461, 2011. doi: 10.1098/rsif.2011.0041.

D. Bluestein et al. Intraluminal thrombus and risk of rupture in patient specific abdominal aortic aneurysm - fsi modelling. *Computer Methods in Biomechanics and Biomedical Engineering*, 12(1):73–81, 2009. doi: 10.1080/10255840802176396.

M.A. Boniforti, L. Di Bella, and R. Magini. On the role of hemodynamics in predicting rupture of the abdominal aortic aneurysm. *Journal of Zhejiang University - Science*, 22(12):957–978, 2021. doi: 10.1631/jzus.A2100308.

E. Bossone and K.A. Eagle. Epidemiology and management of aortic disease: aortic aneurysms and acute aortic syndromes. *Nature Reviews Cardiology*, 18(5):331–348, 2021. doi: 10.1038/S41569-020-00472-6.

A.J. Boyd, D.C.S. Kuhn, R.J. Lozowy, and G.P. Kulbisky. Low wall shear stress predominates at sites of abdominal aortic aneurysm rupture. *Journal of Vascular Surgery*, 63(6):1613–1619, 2016. doi: 10.1016/j.jvs.2015.01.040.

H. Chen, Y. Bi, S. Ju, L. Gu, X. Zhu, and X. Han. Hemodynamics and pathology of an enlarging abdominal aortic aneurysm model in rabbits. *PLoS One*, 13(10):1–11, 2018. doi: 10.1371/journal.pone.0205366.

C.F. Dewey, S.R. Bussolari, M.A. Gimbrone, and P.F. Davies. The dynamic response of vascular endothelial cells to fluid shear stress. *Journal of Biomechanical Engineering*, 103 (3):177–185, 1981. doi: 10.1115/1.3138276.

J.M. Dolan, J. Kolega, and H. Meng. High wall shear stress and spatial gradients in vascular pathology: a review. *Annals of Biomedical Engineering*, 41(7):1411–1427, 2013. doi: 10.1007/s10439-012-0695-0.

B.J. Doyle, T.M. McGloughlin, E.G. Kavanagh, and P.R. Hoskins. From detection to rupture: a serial computational fluid dynamics case study of a rapidly expanding, patient-specific, ruptured abdominal aortic aneurysm. *Computational Biomechanics in Medicine*, 2014. doi: 10.1007/978-1-4939-0745-8_5/FIGURES/8.

B. Ene-Iordache and A. Remuzzi. Disturbed flow in radial-cephalic arteriovenous fistulae for haemodialysis: low and oscillating shear stress locates the sites of stenosis. *Nephrology Dialysis Transplantation*, 27(1):358–368, 2012. doi: 10.1093/ndt/gfr342.

M.F. Fillinger, M.L. Raghavan, S.P. Marra, J.L. Cronenwett, and F.E. Kennedy. In vivo analysis of mechanical wall stress and abdominal aortic aneurysm rupture risk. *Journal of Vascular Surgery*, 36(3):589–597, 2002. doi: 10.1067/MVA.2002.125478.

A. Forneris, F.B. Marotti, A. Satriano, R.D. Moore, and E.S. Di Martino. A novel combined fluid dynamic and strain analysis approach identified abdominal aortic aneurysm rupture. *Journal of Vascular Surgery Cases and Innovative Techniques*, 6(2):172–176, 2020. doi: 10.1016/j.jvscit.2020.01.014.

H.A. Himburg, D.M. Grzybowski, A.L. Hazel, J.A. LaMack, X.M. Li, and M.H. Friedman. Spatial comparison between wall shear stress measures and porcine arterial endothelial permeability. *American Journal of Physiology-Heart and Circulatory Physiology*, 286(5): 1916–1922, 2004. doi: 10.1152/ajpheart.00897.2003.

L.J. Kelsey, J.T. Powell, P.E. Norman, K. Miller, and B.J. Doyle. A comparison of hemodynamic metrics and intraluminal thrombus burden in a common iliac artery aneurysm. *International Journal for Numerical Methods in Biomedical Engineering*, 33(5):1–14, 2017. doi: 10.1002/cnm.2821.

N. Kontopodis, E. Metaxa, Y. Papaharilaou, E. Tavlas, D. Tsetis, and C. Ioannou. Advancements in identifying biomechanical determinants for abdominal aortic aneurysm rupture. *Vascular*, 23(1):65–77, 2015. doi: 10.1177/1708538114532084.

S.W. Lee, L. Antiga, and D.A. Steinman. Correlations among indicators of disturbed flow at the normal carotid bifurcation. *Journal of Biomechanical Engineering*, 131(6):1–7, 2009. doi: 10.1115/1.3127252.

A.S. Les et al. Quantification of hemodynamics in abdominal aortic aneurysms during rest and exercise using magnetic resonance imaging and computational fluid dynamics. *Annals of Biomedical Engineering*, 38(4):1288–1313, 2010. doi: 10.1007/s10439-010-9949-x.

S.N. Lipp et al. Computational hemodynamic modeling of arterial aneurysms: a mini-review. *Frontiers in Physiology*, 11:454, 2020. doi: 10.3389/FPHYS.2020.00454/BIBTEX.

R.J. Lozowy, D.C.S. Kuhn, A.A. Ducas, and A.J. Boyd. The relationship between pulsatile flow impingement and intraluminal thrombus deposition in abdominal aortic aneurysms. *Cardiovascular Engineering and Technology*, 8(1):57–69, 2017. doi: 10.1007/s13239-016-0287-5.

A.M. Malek. Hemodynamic shear stress and its role in atherosclerosis. *JAMA*, 282(21): 2035, 1999. doi: 10.1001/jama.282.21.2035.

D.B. McClarty, D.C.S. Kuhn, and A.J. Boyd. Hemodynamic changes in an actively rupturing abdominal aortic aneurysm. *Journal of Vascular Research*, 58(3):172–179, 2021. doi: 10.1159/000514237.

T.M. McGloughlin and B.J. Doyle. New approaches to abdominal aortic aneurysm rupture risk assessment: engineering insights with clinical gain. *Arteriosclerosis, Thrombosis, and Vascular Biology*, 30(9):1687–1694, 2010. doi: 10.1161/ATVBAHA.110.204529.

H. Meng, V.M. Tutino, J. Xiang, and A. Siddiqui. High wss or low wss? complex interactions of hemodynamics with intracranial aneurysm initiation, growth, and rupture: toward a unifying hypothesis. *American Journal of Neuroradiology*, 35(7):1254–1262, 2014. doi: 10.3174/ajnr.A3558.

H. Meng et al. Complex hemodynamics at the apex of an arterial bifurcation induces vascular remodeling resembling cerebral aneurysm initiation. *Stroke*, 38(6):1924–1931, 2007. doi: 10.1161/STROKEAHA.106.481234.

E. Metaxa, H. Meng, S.R. Kaluvala, M.P. Szymanski, R.A. Paluch, and J. Kolega. Nitric oxide-dependent stimulation of endothelial cell proliferation by sustained high flow. *American Journal of Physiology-Heart and Circulatory Physiology*, 295(2):736–742, 2008. doi: 10.1152/ajpheart.01156.2007.

E. Metaxa, K. Tzirakis, N. Kontopodis, C.V. Ioannou, and Y. Papaharilaou. Correlation of intraluminal thrombus deposition, biomechanics, and hemodynamics with surface growth and rupture in abdominal aortic aneurysm—application in a clinical paradigm. *Annals of Vascular Surgery*, 46:357–366, 2018. doi: 10.1016/j.avsg.2017.08.007.

Onur Mutlu, Huseyin Enes Salman, Hassan Al-Thani, Ayman El-Menyar, Uvais Ahmed Qidwai, and Huseyin Cagatay Yalcin. How does hemodynamics affect rupture tissue mechanics in abdominal aortic aneurysm: Focus on wall shear stress derived parameters, time-averaged wall shear stress, oscillatory shear index, endothelial cell activation potential, and relative residence time. *Computers in Biology and Medicine*, 154:106609, 2023. ISSN 0010-4825. doi: https://doi.org/10.1016/j.compbiomed.2023.106609.

M. Okano and Y. Yoshida. Junction complexes of endothelial cells in atherosclerosis-prone and atherosclerosis-resistant regions on flow dividers of brachiocephalic bifurcations in the rabbit aorta. *Biorheology*, 31(2):155–161, 1994. doi: 10.3233/BIR-1994-31203.

M.J. O'Rourke, J.P. McCullough, and S. Kelly. An investigation of the relationship between hemodynamics and thrombus deposition within patient-specific models of abdominal aortic aneurysm. *Proceedings of the Institution of Mechanical Engineers, Part H: Journal of Engineering in Medicine*, 226(7):548–564, 2012. doi: 10.1177/0954411912444080.

J.J. Paszkowiak and A. Dardik. Arterial wall shear stress: observations from the bench to the bedside. *Vascular and Endovascular Surgery*, 37(1):47–57, 2003. doi: 10.1177/153857440303700107.

S. Polzer and T.C. Gasser. Biomechanical rupture risk assessment of abdominal aortic aneurysms based on a novel probabilistic rupture risk index. *Journal of the Royal Society Interface*, 12, 2015. doi: 10.1098/RSIF.2015.0852.

Y. Qiu et al. Role of intraluminal thrombus in abdominal aortic aneurysm ruptures: a hemodynamic point of view. *Medical Physics*, 46(9):4263–4275, 2019. doi: 10.1002/mp.13658.

R.S. Reneman, T. Arts, and A.P.G. Hoeks. Wall shear stress–an important determinant of endothelial cell function and structure–in the arterial system in vivo. discrepancies with theory. *Journal of Vascular Research*, 43(3):251–269, 2006. doi: 10.1159/000091648.

N. Sakalihasan, R. Limet, and O. Defawe. Abdominal aortic aneurysm. *The Lancet*, 365 (9470):1577–1589, 2005. doi: 10.1016/S0140-6736(05)66459-8.

H.E. Salman, B. Ramazanli, M.M. Yavuz, and H.C. Yalcin. Biomechanical investigation of disturbed hemodynamics-induced tissue degeneration in abdominal aortic aneurysms using computational and experimental techniques. *Frontiers in Bioengineering and Biotechnology*, 7:111, 2019. doi: 10.3389/fbioe.2019.00111.

H.E. Salman, L. Saltik, and H.C. Yalcin. Computational analysis of wall shear stress patterns on calcified and bicuspid aortic valves: focus on radial and coaptation patterns. *Fluids*, 6(8), 2021. doi: 10.3390/FLUIDS6080287.

U.K.A. Sampson et al. Global and regional burden of aortic dissection and aneurysms: mortality trends in 21 world regions, 1990 to 2010. *Global Heart*, 9(1):171–180.e10, 2014. doi: 10.1016/J.GHEART.2013.12.010.

M. Shojima. Magnitude and role of wall shear stress on cerebral aneurysm. computational fluid dynamic study of 20 middle cerebral artery aneurysms. *Stroke*, 2004. doi: 10.1161/01.str.0000144648.89172.of.

H. Si. Tetgen, a delaunay-based quality tetrahedral mesh generator. *ACM Transactions on Mathematical Software*, 41(11), 2015.

M.P. Szymanski, E. Metaxa, H. Meng, and J. Kolega. Endothelial cell layer subjected to impinging flow mimicking the apex of an arterial bifurcation. *Annals of Biomedical Engineering*, 36(10):1681–1689, 2008. doi: 10.1007/s10439-008-9540-x.

C.A. Taylor, T.J.R. Hughes, and C.K. Zarins. Finite element modeling of three-dimensional pulsatile flow in the abdominal aorta: relevance to atherosclerosis. *Annals of Biomedical Engineering*, 26(6):975–987, 1998. doi: 10.1114/1.140.

C.A. Taylor, T.J.R. Hughes, and C.K. Zarins. Effect of exercise on hemodynamic conditions in the abdominal aorta. *Journal of Vascular Surgery*, 29(6):1077–1089, 1999. doi: 10.1016/S0741-5214(99)70249-1.

K. Tzirakis, Y. Kamarianakis, E. Metaxa, N. Kontopodis, C.V. Ioannou, and Y. Papaharilaou. A robust approach for exploring hemodynamics and thrombus growth associations in abdominal aortic aneurysms. *Medical and Biological Engineering and Computing*, 55 (8):1493–1506, 2017. doi: 10.1007/s11517-016-1610-x.

D.A. Vorp et al. Association of intraluminal thrombus in abdominal aortic aneurysm with local hypoxia and wall weakening. *Journal of Vascular Surgery*, 34(2):291–299, 2001. doi: 10.1067/MVA.2001.114813.

X. Wang and X. Li. A fluid-structure interaction-based numerical investigation on the evolution of stress, strength and rupture potential of an abdominal aortic aneurysm. *Computer Methods in Biomechanics and Biomedical Engineering*, 16(9):1032–1039, 2013. doi: 10.1080/10255842.2011.652097.

P.N. Watton, N.B. Raberger, G.A. Holzapfel, and Y. Ventikos. Coupling the hemodynamic environment to the evolution of cerebral aneurysms: computational framework and numerical examples. *Journal of Biomechanical Engineering*, 131(10):1–14, 2009. doi: 10.1115/1.3192141.

T.B.M. Wilmink, C.R.G. Quick, C.S. Hubbard, and N.E. Day. The influence of screening on the incidence of ruptured abdominal aortic aneurysms. *Journal of Vascular Surgery*, 30(2):203–208, 1999. doi: 10.1016/S0741-5214(99)70129-1.

M. Xenos et al. Patient-based abdominal aortic aneurysm rupture risk prediction with fluid structure interaction modeling. *Annals of Biomedical Engineering*, 38(11):3323–3337, 2010. doi: 10.1007/s10439-010-0094-3.

J. Xiang et al. Hemodynamic-morphologic discriminants for intracranial aneurysm rupture. *Stroke*, 42(1):144–152, 2011. doi: 10.1161/STROKEAHA.110.592923.

B.A. Zambrano, H. Gharahi, C.Y. Lim, W. Lee, and S. Baek. Association of vortical structures and hemodynamic parameters for regional thrombus accumulation in abdominal aortic aneurysms. *International Journal for Numerical Methods in Biomedical Engineering*, 2021. doi: 10.1002/cnm.3555.

B.A. Zambrano et al. Association of intraluminal thrombus, hemodynamic forces, and abdominal aortic aneurysm expansion using longitudinal ct images. *Annals of Biomedical Engineering*, 44(5):1502–1514, 2016. doi: 10.1007/s10439-015-1461-x.